Journal of the Oceanographical Society of Japan
Vol. 38, pp. 313 to 322, 1982

Internal Flow Structure of Short Wind Waves
Part II. The Streamline Pattern*

Kuniaki OKUDA**

Abstract: Characteristic features of the internal flow field of short wind waves are described mainly on the basis of streamline patterns measured for four different cases of individual wave. In some waves a distinct high vorticity region, with flow in excess of the phase speed in the surface thin layer, is formed near the crest as shown in Part I of this study, but the streamlines are found to remain quite regular even very near the water surface. The characteristics of flow in the high vorticity region are investigated, and it is argued that the high vorticity region is not supported steadily in individual waves but that growth and attenuation in individual waves repeats systematically, without no severe wave breaking. Below the surface vorticity layer a quite regular wave motion dominates. However, this wave motion is strongly affected by the presence of the high vorticity region. By comparing the measured streamline profiles with those predicted from wave profiles by the use of a water-wave theory, it is found that the flow of the wind waves studied cannot be predicted, even approximately, from the surface displacements, in contrast to the case of pure irrotational water waves.

1. Introduction

In Part I of this study (OKUDA, 1982) characteristic features of the internal vorticity distribution relative to the individual wave crests of short wind waves were described. The most interesting feature found in Part I is that distinct waves, waves with wave height comparable with or larger than the mean, in the field possess high vorticity regions below the crests, extending from the water surface to a depth of about one third of the wave height. On the basis of the measured tangential stress distribution and the internal velocity field near the crest, it was argued that the high vorticity region of distinct waves is associated with the local generation of vorticity by the intense tangential stress near individual crests.

In Part I (OKUDA, 1982) the detailed flow structure associated with this high vorticity region was the main topic of discussion. In the present article (Part II) characteristic features of the overall flow field, including the inner substantially irrotational region below the surface vorticity layer, are described. The experimental conditions and the characteristic values of the four different cases of individual wave measured (Cases I~IV) have been presented in a previous article (Part I).

* Received Mar. 6, 1981, revised Apr. 6 and accepted Sept. 1, 1982.

** Geophysical Institute, Faculty of Science, Tohoku University, Sendai 980, Japan

2. Method of calculation of streamlines

To specify position relative to the wave profile, an orthogonal Cartesian coordinate system (x, y, z) which is moving with the phase speed is used, where x is the horizontal distance measured along the downstream direction, y is the distance along the lateral direction, and z is the distance along the vertical direction taken upward. Since the flow being studied is approximately two-dimensional in the $x-z$ plane as mentioned in a previous article (Part I), streamline patterns of individual waves are calculated from measured U (x-component) and W (z-component).

In the moving frame used here, the stream function $\Psi'(x, z)$ is defined as

$$\frac{\partial \Psi'}{\partial x} = -W,$$

$$\frac{\partial \Psi'}{\partial z} = -C+U$$

where C is the phase speed. By integrating these equations, we obtain

$$\Psi(x_1, z_1) \equiv \Psi'(x_1, z_1) - \Psi'(x_0, z_0)$$
$$= \left[\int_{z_0}^{z_1} (-C+U)dx\right]_{x=x_1} + \left[\int_{x_0}^{x_1} -W dx\right]_{z=z_1},$$

where $[\quad]_{x=x_1}$ and $[\quad]_{z=z_1}$ indicate the integrations along $x=x_1$ and $z=z_1$, respectively, and $\Psi'(x_0, z_0)$ is an integral constant. The streamlines are the lines of equal values of $\Psi(x_1, z_1)$. If the flow field of individual waves are disturbed by local occurrences of turbulence which is inevitably three-dimensional, the patterns of the streamlines may vary depending on the choice of integration paths. Therefore, $\Psi(x_1, z_1)$ was calculated along various integration paths, and the constancy of the pattern of streamlines was confirmed.

3. Results and discussion

3.1. Streamline patterns

Streamline patterns observed in a frame of reference moving with the wave profile are shown in Fig. 1. The numbers on streamlines are the values of Ψ ($cm^2 s^{-1}$). For Cases I, II and III streamlines are not drawn for the region near the crest due to the lack of flow measurements. Every streamline shown here is directed from right to left. As described in Part I of this study (OKUDA, 1982), the overall flow field of each wave was constructed from a series of measurements made while the wave passed

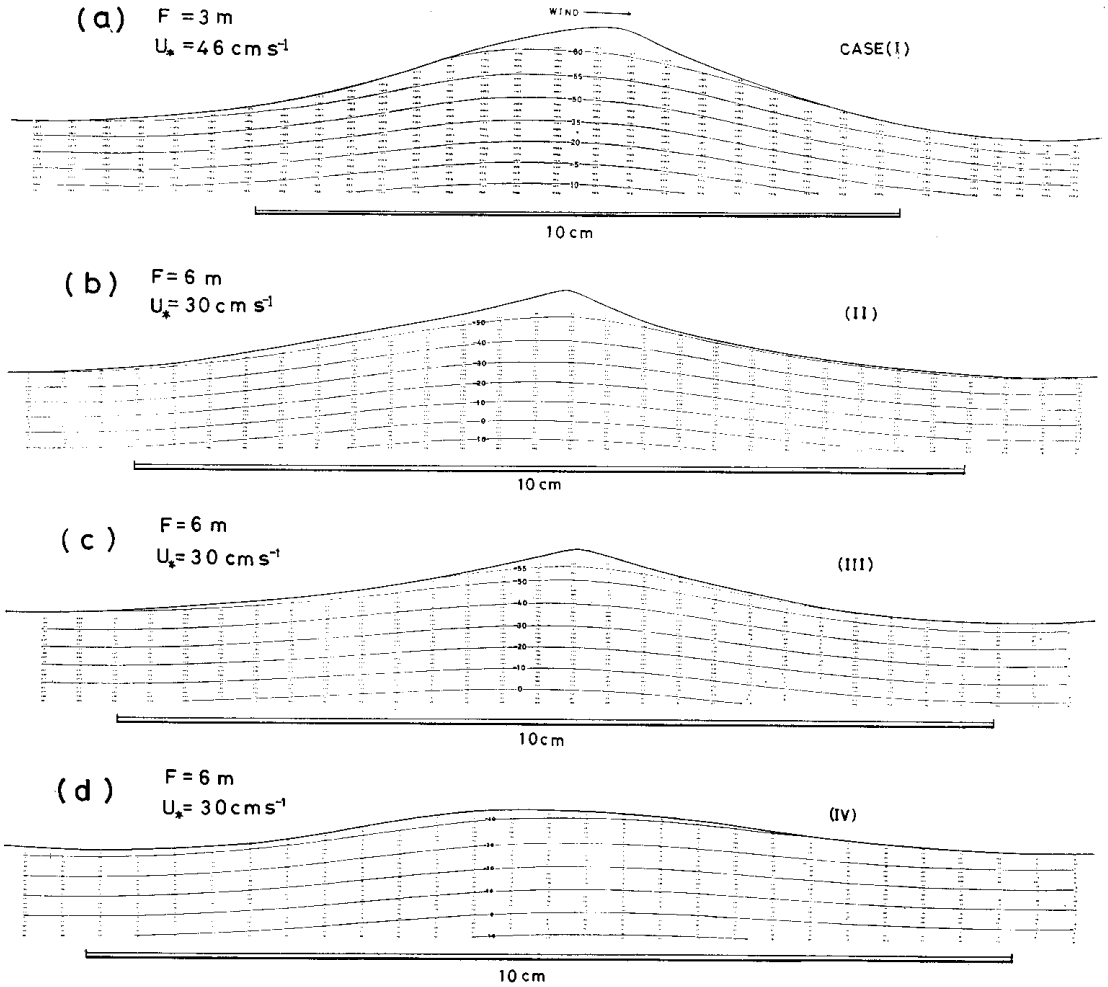

Fig. 1. Steamlines in a frame of reference moving with the wave profile. Every streamline shown is directed upwind.

the observation area. The streamline patterns shown here, however, can be regarded to represent approximately the instantaneous flow patterns of each waves, since the variation of the flow pattern in such a short time period is evidently small (this will be confirmed in Section 3.3.). Because of the weakness of the unsteady motion, the streamlines shown here also approximately indicate path lines of water elements relative to the wave profile; this assertation may become invalid near the crests for Cases I, II and III, since, as shown in a previous article (Part I), the flow velocity in this moving frame is close to zero at such points so that the unsteady motion, even if it is weak, significantly affects the streamline pattern.

For every case streamlines are quite smooth. According to the investigations of Part I, the vorticity is extremely high near the crest for Cases I, II and III, and the flow in the surface thin layer on the top of the high vorticity region is in excess of the phase speed. For Case II, in particular, the occurrence of downward intrusion of water elements just leeward of the crest (wave breaking in a wide sense) was indicated. However, in this case (Case II), the streamline even just below the water surface ($\Psi=-50$) is quite smooth. This indicates that the flow of wind waves, in both the surface vorticity layer and the inner irrotational part, is well-organized, and no particularly intense turbulent motion is occurring in spite of the presence of excess flow.

The streamline patterns for Cases I, II and III, however, show a noticeable difference from that of irrotational gravity waves. From the streamlines shown here, taken together with their vorticity distributions (an enlarged section of fig. 3 in Part I: OKUDA, 1982, is shown in Fig. 2), it is seen that near the crest, streamlines pass along the lines of equal vorticity rather than along the water surface. The streamlines of $\Psi=-80$ for Case I, -50 for Case II and -55 for Case III appear to define approximately the lower boundary of the high vorticity region. An explanation for this may be offered from the fact that the streamlines shown here approximately coincide with path lines. Even at the depth where the uppermost streamlines pass, the flow velocity is much smaller than the phase speed. The water elements are therefore convected, in the moving frame, from the leeside to the windward side of the crest in a very short time. Consequently, it is considered that water elements pass by below the high vorticity region retaining most of their vorticity. The streamlines thus coincide approximately with the lines of equal vorticity.

3.2. The unsteadiness of flow in the high vorticity region

The streamlines just below the water surface, ($\Psi=-80$ for Case I, -50 for Case II and -55 for Case III) appear to separate the high vorticity region near the crest from the lower region. Let us now discuss the streamline pattern formed in the high vorticity region.

As mentioned in Part I of this study (OKUDA, 1982), the high vorticity region has a thin surface layer in which the flow is in excess of the phase speed. The steady state streamline pattern resulting from this type of flow under the assumption of the steadiness of flow together with the features of streamline patterns shown in Fig. 1, should be of "closed-loops type", similar to that proposed for mean streamlines of breaking waves by PHILLIPS (1977). This flow pattern implies that the forward mass flux near the water surface is in balance with the backward mass flux below the excess flow layer, hence a strong downward intrusion results a little leeward of the crest. However, it is evident that such a flow contradicts the present measurements. Figure 2 shows, superimposed on the vorticity distributions, velocity vectors below the lee face for Cases II and III. Four groups of instantaneous measurements are shown alternately by dashed and solid arrows. The surface vorticity layer for Case II is interrupted a little leeward of the crest, which indicates the occurrence of the intrusion mentioned in Part I (OKUDA, 1982: sect. 3.1.). The velocity vectors, however, show a regular pattern even very near the water surface, which suggests that the intrusion is weak and its direct influence is limited to a very small region near the intrusion point. This is also indicated by the smoothness of $\Psi=-50$ in Fig. 1b. The velocity vectors also show a quite regular pattern for Case III, and, in this case, the surface vorticity layer is not interrupted. This indicates that the intrusion is not occurring, in spite of the

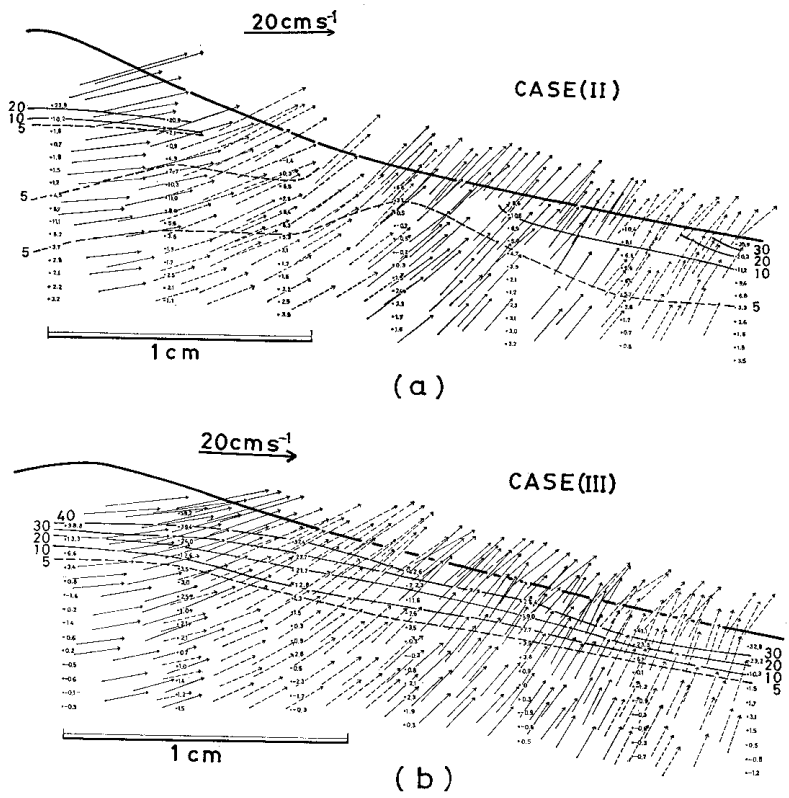

Fig. 2. Velocity vectors near the water surface in the region from the crest up to a certain point on the leeside of the crest for Cases II and III. Arrows represent the flow velocities indicated at their tails. Numerals next to the small dots indicate values of vorticity, and lines of equal vorticity are also shown by solid and dashed lines.

presence of the high vorticity region and the associated excess flow. These features show that the streamline pattern in the high vorticity region differs from the "closed-loops type" which is predicted from the assumption of the steadiness of flow.

The flow in the high vorticity region seems to be intrinsically unsteady. According to HATORI (1981), the wave height of individual waves varies significantly in both space and time with some periodicity, and the variational pattern propagates with the group velocity. As shown in Part I (OKUDA, 1982: sect. 3.2.), the high vorticity region is found in distinct waves (i.e. waves of large wave height near or at the crest of the modulated wave patterns), but usually not in waves with small wave height (i.e. those near or at the trough of the modulated wave pattern). This suggests that, since individual waves propagate faster than the modulated wave pattern with the phase speed, the high vorticity region is repeating the growth and the attenuation in the individual waves as they propagate in space.

The above mentioned features of flow in the high vorticity region are also predicted from the following considerations. Let us concentrate on the vorticity distribution for Case II (Fig. 2a) and assume, tentatively, that the lines of same vorticity drawn in this figure coincide with path lines observed in a frame of reference moving with the wave profile. Under this assumption the following is evident. The water elements moving along the lee face toward the crest cannot penetrate into the high vorticity region below the crest, therefore, there is no mass flux into the high vorticity region from the leeside. On the other hand, water elements with large vorticity in the high vorticity region leak out along the windward face, since even

in the high vorticity region the flow velocity is smaller than the phase speed except for the very thin surface layer. Thus, the high vorticity region in Case II is attenuating. In fact, the vorticity distributions of Case II (fig. 3b in Part I: OKUDA, 1982), show the existence of a very distinct surface vorticity layer below the windward face, though the surface vorticity layer dissipates below the lee face. In Part I (OKUDA, 1982: sect. 3.2.), it was confirmed that the waves with internal flow fields similar to that of Case II (the waves with flow type Z: OKUDA, 1982) exist generally in the wind wave field. This suggests that the attenuation of the high vorticity region is a general feature. Evidently, growth of the high vorticity region should occur in some waves, or in advance of the beginning of attenuation. In Part I the existence of waves which accompany the excess flow but do not have downward intrusion a little leeward of the crest (the waves with flow type Y: OKUDA, 1982), was also confirmed; Case III is a typical example of this type of waves. Growth of the high vorticity region may occur in these waves. For Case III the streamline $\Psi=-55$ (see Fig. 1c) starts from a point considerably ahead of the crest and terminates a little windward of the crest, and it has been shown that the surface vorticity layer is more distinct below the lee face than the windward face in Part I of this study (OKUDA, 1982:

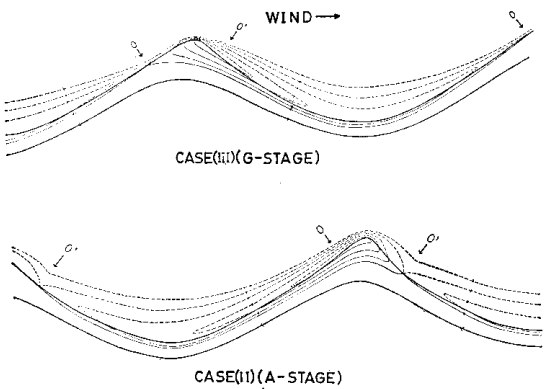

Fig. 3. Proposed streamlines near the water surface for Cases III and II. Solid line: streamline in water; dashed line: steamline in air; thick solid line below the water surface: streamline which passes through the inner irrotational region; 0 and 0′: the point where the horizontal component of the surface velocity is zero.

fig. 3c). These facts seem to indicate that rising of the water surface near the crest occurs associated with the net accumulation of water elements with high vorticity below the crest.

Figure 3 shows, for Cases II and III, the streamline patterns near the water surface predicted from the above discussion together with some other kinematical features. For Case III the high vorticity region is in the growth stage (G-stage in Fig. 3), and for Case II in the attenuation stage (A-stage in Fig. 3). Streamlines in water are indicated by solid lines and those in air, determined to fit the internal streamlines, by dashed lines. A thick solid line below the water surface indicates a streamline which passes through the inner irrotational region. 0 and 0′ indicate the points where the horizontal component of the surface velocity is zero in the moving frame. It may be noted that streamlines shown here, especially those near the crest where unsteady motion is relatively dominant, may differ considerably from the path lines; some characteristic features of particle movements near the crest of distinct waves have been described in Part I of this study (OKUDA, 1982: sect. 3.2.). Streamline patterns shown here have the following features:

(i) They differ in pattern from the steady flow pattern proposed by PHILLIPS (1977) and, for the air flow proposed by BANNER and MELVILLE (1976) and GENT and TAYLOR (1977), in that the regions of closed streamlines bounded by the water surface do not appear in both air and water.

(ii) In Case III the streamline which terminates at 0 passes a little below 0′, which indicates the occurrence of net inflow into the high vorticity region in this instance (this does not mean the water between this streamline and the water surface is entirely trapped in the high vorticity region, because the streamline and the path line differ in the unsteady flow being studied). In Case II the streamline which starts at 0′ passes a little below 0, which indicates the occurrence of net leakage out of the high vorticity region.

(iii) In Case III the velocity component normal to the water surface is outward around the crest (between 0 and 0′), and is inward in other regions, which indicates that the wave steepness is increasing associated with the growth

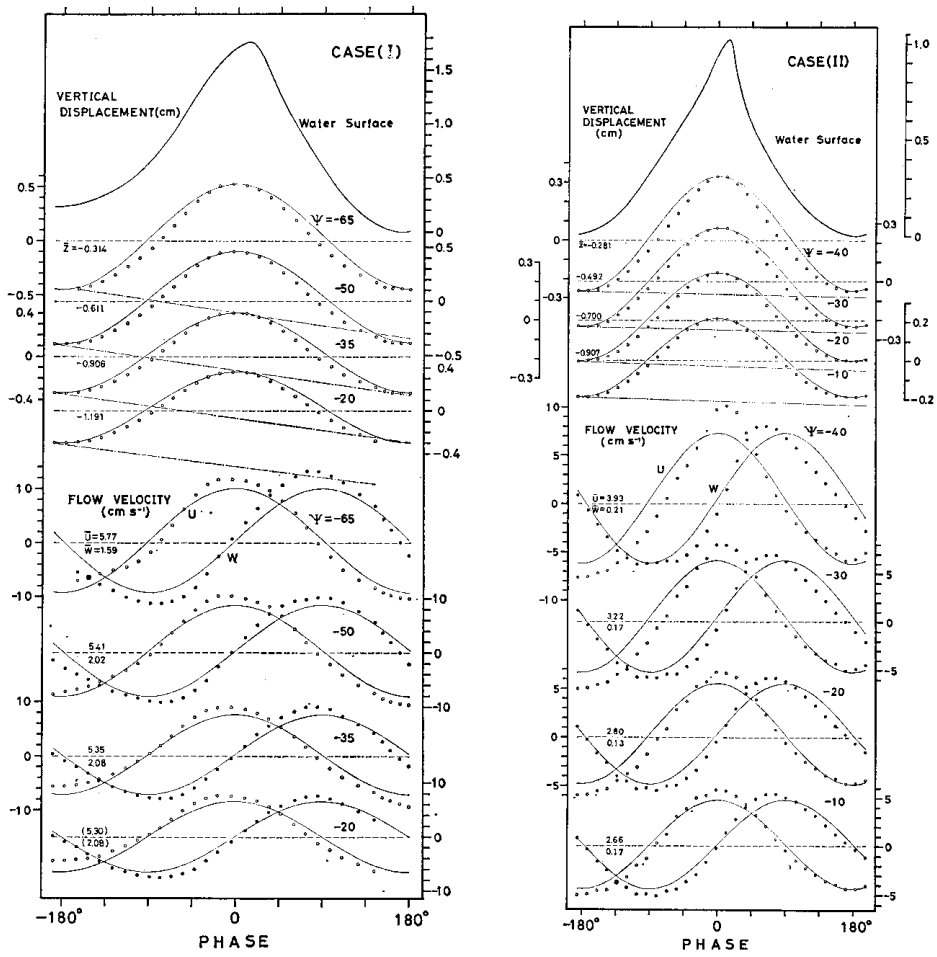

Fig. 4. Streamline profiles and velocity distributions along the streamlines. The abscissa→

of the high vorticity region. In Case II, contrary to Case III, the wave steepness is decreasing, associated with the attenuation of the high vorticity region.

(iv) In Case III 0′ is not a stagnation point, which indicates that 0′ is neither the intrusion point of water nor the separation point of air flow. In Case II 0′ is a stagnation point, which indicates the occurrence of both intrusion and separation.

These four features of supposed streamlines are very consistent with the actual measurements in this study.

3.3. *The characteristics of the motion below the surface vorticity layer*

Some characteristics of flow below the surface vorticity layer can be seen from Fig. 4. Each part of this figure contains, from the top, the wave profile, the profiles of some streamlines and the velocity distributions along the respective streamlines. Every streamline, except $\Psi=-30$ for Case IV, passes, through the region where the vorticity is practically zero, as shown in Part I of this study (OKUDA, 1982: fig. 3). The abscissa represents the phase defined as $-180°$ at the windward trough and 180° at the leeward trough; the peak of the wave profile is not necessarily 0°. The value of $\bar{Z}$ shown for each streamline profile indicates the mean depth in cm. $\bar{U}$ and $\bar{W}$ are the averages of the horizontal component U and the vertical component W over the region between $-180°$ and 180°, respectively. For each wave $\bar{W}$ does not necessarily vanish. The flow velocity was measured by tracing of hydrogen bubles as

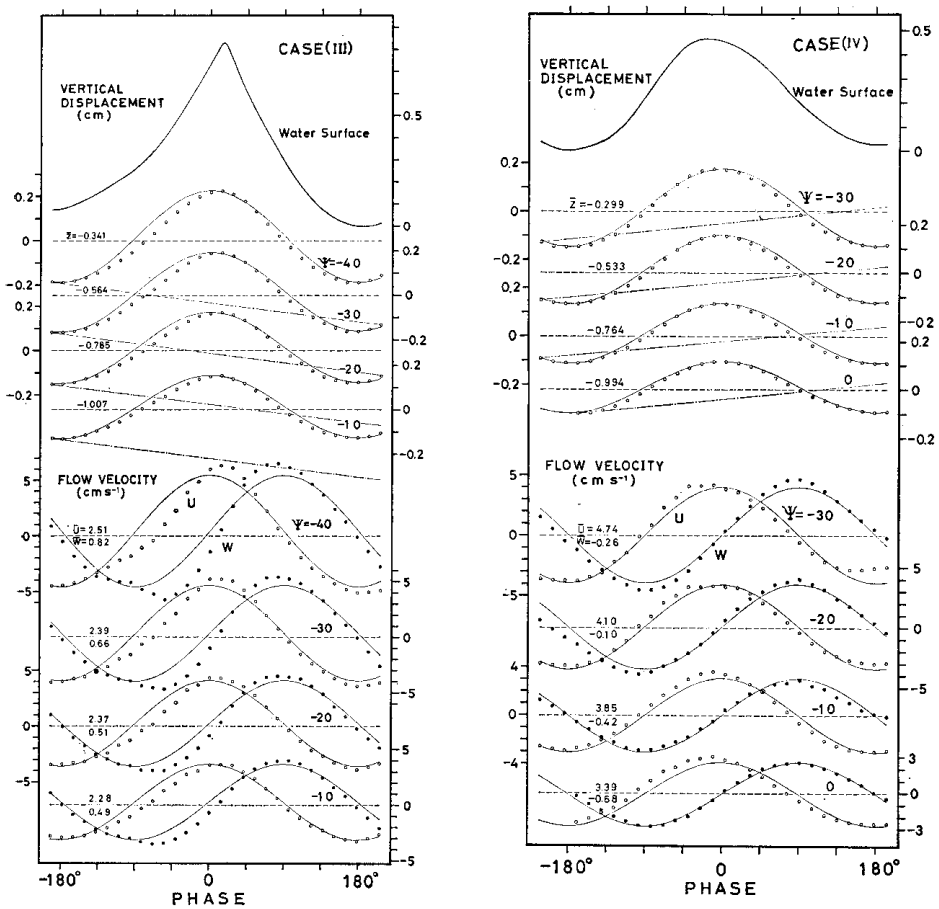

→represents the phase defined as $-180°$ at the windward trough and $180°$ at the leeward trough; $\bar{Z}$: mean depth of streamline; $\bar{U}$ and $\bar{W}$: averages over a wavelength of U and W, respectively; solid line: the sinusoid with amplitude of the individual streamline (vertical displacement) and with amplitude $a(gk)^{1/2}$, where a is the amplitude of streamline, g is the gravitational acceleration and k is the wave number (flow velocity); inclined dash-dot line: the drift.

described in Part I of this study (OKUDA, 1982: sect. 2). In Cases I and III $\bar{W}$ is larger than the value predicted from the ascent velocity of bubbles (smaller than $0.2\,\mathrm{cm\,s^{-1}}$) and for Case IV it is in the opposite direction to the ascent velocity. Corresponding to the existence of $\bar{W}$, the streamline which starts at 180° fails to return to its original depth at $-180°$. This may be caused by the unsteadiness of flow mentioned in the previous section, and it may also be caused by the non-uniformity of the wave train. The vertical drift of the streamline shown by the inclined dash-dot lines, however, is, at the most, comparable in extent to the amplitude of the respective streamlines so that the presence of vertical drift will have little bearing on the following discussion.

The wave profiles, especially for Cases I, II and III, have very steep wave crests and also distinct asymmetry with respect to the crest. However, even for these the streamline profiles can be approximately fitted by solid sinusoidal lines having the amplitudes of individual streamlines. If the streamline profiles for Cases I, II and III are examined in more detail, we can certainly find some deformations from the sinusoid somewhat similar to that in the wave profile, but deformation is very small. In Fig. 5, as an example, the observed profile of $\Psi = -40$ for Case II (open circles) is compared with

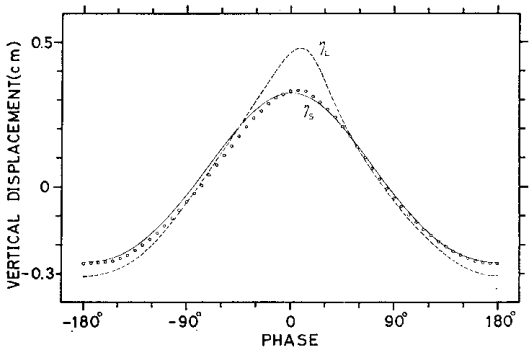

Fig. 5. A comparison of the observed profile of $\Psi=-40$ for Case II (open circles) with η_L and η_S.

the profile η_L, which is predicted at the mean depth of $\Psi=-40$ under the assumption that the wave profile of Case II is a resultant of the linear superposition of its Fourier components. The difference is large. In the figure a third order Stokes' profile estimated from the amplitude of the dominant component of the streamline profile η_S is also shown. The observed profile fits very well to the Stokes' profile, except that the observed profile has a slightly steeper crest and a slight asymmetry with respect to the crest.

For the velocity distributions along streamlines, the sinusoids with amplitudes $a(gk)^{1/2}$, where a is the amplitude of the streamline, g is the gravitational acceleration, and k is the wave number, are drawn in Fig. 4. The amplitude of the observed velocity distributions seems to be a little greater than $a(gk)^{1/2}$, especially for Cases I, II and III. For some distributions, in addition to some systematic deformations from the sinusoid which correspond to the deformations found in the streamline profile mentioned above, we can detect irregular variations occurring rather locally; for example, for Case II U for $\Psi=-40$ and -30 shows particularly large values near the crest, which is caused by the passing of streamlines across the region of high vorticity which penetrates deep below the crest as indicated by the line of $\omega=5$ (see OKUDA, 1982: fig. 3b). However, the present results evidently indicate that regular wave motion dominates below the surface vorticity layer.

Some characteristic features of wave motion in the inner region are summarized in Table 1.

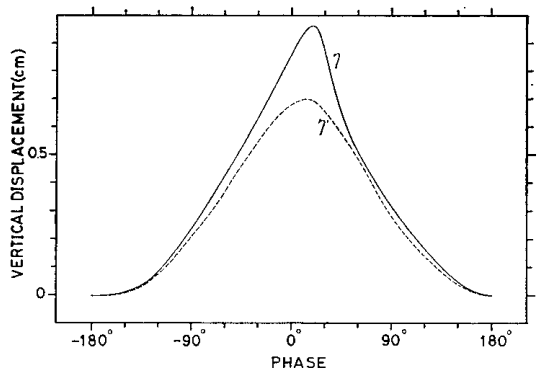

Fig. 6. A comparison of the observed wave profile (η) for Case II with the profile obtained by extrapolating $\Psi=-40$ for Case II up to the mean water surface level (η').

Listed in the columns for the vertical displacements are (i) the observed amplitude of respective streamlines a, (ii) the amplitude calculated by the equation

$$a'=a_m e^{k(\bar{z}-\bar{z}_m)},$$

where a_m and $\bar{z}_m$ are respectively the observed amplitude and the mean depth of the streamline which passes at the deepest point of each waves, and (iii) $2a'_0/H$ where H is the wave height of individual waves and a'_0 is the value of a' at $\bar{z}=0$. For every case a coincides closely with a', which means that the amplitude of the streamline in the inner region follows quite closely an exponential decrease with increase of depth. The values of $2a'_0/H$ are almost the same for Cases I, II and III but are considerably smaller than unity (about 0.65). The implications of this value are revealed by Fig. 6. The observed wave profile for Case II is shown by η, and the profile obtained by extrapolating the amplitudes of individual Fourier components of the profile for $\Psi=-40$ exponentially up to the mean water surface level ($\bar{z}=0$) is shown by η'. It is considered that η' is the virtual water surface for the motion of the inner region, and, if we take into consideration the fact that the streamlines a little below the water surface approximately pass along the lines of equal vorticity as mentioned before, then η' also approximately defines the lower boundary of the high vorticity region near the crest. The wave height of η is H and that of η' is $2a'_0$. The value obtained by subtracting $2a'_0$ from H

Table 1. Characteristic values of wave motion in the inner region.

		$\bar{Z}$(cm)	Vertical displacement(cm) Amplitude a(obs.)	a'	$2a_0'/H$	U(cm s^{-1}) Amplitude $\tilde{U}$(obs.)	$a\sigma$	$\tilde{U}/a\sigma$	W(cm s^{-1}) Amplitude $\tilde{W}$(obs.)	$\tilde{W}/a\sigma$	Drift(cm s^{-1}) U_L	σka^2
Case (I)	$\Psi=-65$	−0.31	0.49	0.47		10.45	9.67	1.08	12.27	1.27	—	1.89
$k=0.40$	−50	−0.61	0.43	0.42	0.65	9.60	8.45	1.14	9.71	1.15	1.68	1.44
$H=1.64$	−35	−0.91	0.37	0.37		8.15	7.37	1.11	8.48	1.15	1.30	1.10
	−20	−1.19	0.33	—		(6.86)	6.58	1.04	7.59	1.15	—	0.87
Case (II)	$\Psi=-40$	−0.28	0.30	0.28		8.51	6.76	1.26	7.18	1.06	—	1.07
$k=0.53$	−30	−0.49	0.26	0.25	0.64	7.00	5.81	1.20	6.37	1.10	0.89	0.79
$H=1.01$	−20	−0.70	0.23	0.22		6.04	5.20	1.16	5.80	1.12	0.66	0.63
	−10	−0.91	0.20	—		5.30	4.60	1.15	5.24	1.14	0.63	0.49
Case (III)	$\Psi=-40$	−0.34	0.21	0.21		5.59	5.04	1.11	6.10	1.21	—	0.63
$k=0.60$	−30	−0.56	0.18	0.18	0.65	4.78	4.33	1.10	5.08	1.17	0.48	0.46
$H=0.79$	−20	−0.79	0.16	0.16		4.02	3.86	1.04	4.26	1.10	0.32	0.37
	−10	−1.01	0.14	—		3.40	3.43	0.99	3.75	1.09	0.33	0.29
Case (IV)	$\Psi=-30$	−0.30	0.16	0.17		3.75	3.99	0.94	4.61	1.16	—	0.40
$k=0.63$	−20	−0.53	0.14	0.15	0.91	3.31	3.52	0.94	3.94	1.12	0.19	0.31
$H=0.45$	−10	−0.76	0.12	0.13		3.27	3.06	1.07	2.91	0.95	0.30	0.24
	0	−0.99	0.11	—		2.82	2.65	1.06	2.66	1.00	0.12	0.18

thus represents the thickness of the high vorticity region near the crest. For Case IV $2a'_0/H$ is close to unity, which is due to the fact that the region where the vorticity is particularly high is not so distinct as in the other cases.

Listed in the columns for U and W in Table 1 are (i) the values of the observed amplitude $\tilde{U}$ and $\tilde{W}$, (ii) the values of $a\sigma$ where $\sigma=(gk)^{1/2}$, and (iii) the ratio of (i) and (ii). The observed amplitude is evidently larger than $a\sigma$, especially for Cases I, II and III. Their mean ratio calculated from the values for Cases I, II and III is 1.12; the values for distributions showing irregular variations, for example U for $\Psi=-40$ and -30 of Case II mentioned above, are excluded. This value may indicate that the dispersion relation of wind waves is modified by the presence of the high vorticity region near the crest, and this will be confirmed in Part III of this study (OKUDA, MS).

In the columns for drift, the values of mean particle speed (Stokes' drift) obtained by two different methods are shown. One was calculated from the observed amplitude of respective streamlines by σka^2, and the other ($\bar{U}_L$) was obtained in the following manner. In a frame of reference moving with the waves, water particles move along streamlines from leeside to the windward side of the crest. The time needed for moving a distance of one wavelength is

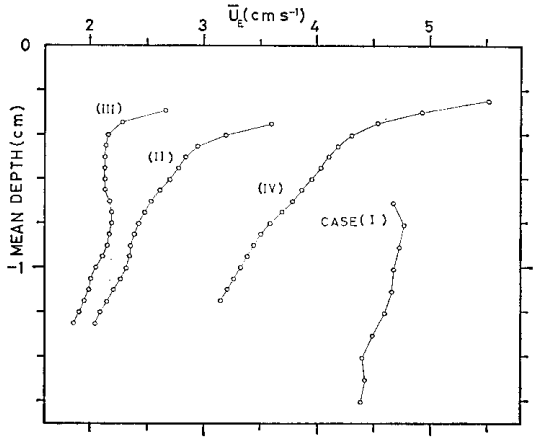

Fig. 7. Profiles of mean flow velocity measured at fixed depths from the mean water surface level.

$$T_P=\int^{L}\frac{dx}{C-U},$$

where the integration is performed along the the streamlines. The mean particle speed in this moving frame is $-L/T_P$, consequently, it is $C-L/T_P$ in the spatially fixed frame. We now consider the mean particle speed induced by the wave motion, which is obtained by subtracting the mean flow velocity from the above at the mean depth of the streamline. Thus, denoting the mean flow velocity as $\bar{U}_E$, $\bar{U}_L$ is given by

$$\bar{U}_L = C - L/T_P - \bar{U}_E .$$

The observed profiles of $\bar{U}_E$ for respective waves are shown in Fig. 7. The values obtained by this method agree well with the calculations of σka^2.

The above discussion suggests that the flow below the surface vorticity layer strongly possesses the characteristics of regular irrotational waves, in spite of the presence of the high vorticity region near the crest and the excess flow. While the present results simultaneously indicate that the wave motion is strongly influenced by the presence of the vorticity region near the crest, so that the internal streamline pattern cannot be known, even approximately, from surface displacements alone, contrary to the case of irrotational waves. Our previous flow visualization studies (TOBA *et al.*, 1975; OKUDA *et al.*, 1976) showed the existence of intense rotational motion with a downward component on the leeside of the crest and an upward component on the windward side, called 'forced convection'. In these studies the existence of 'forced convection' was identified from the great intensity of the measured flow velocity minus the irrotational motion estimated from the wave profile. By measuring flow with anemometer IMASATO and ICHIKAWA (1977) also detected an intense coherent motion moving with the wave profile, called 'coherent turbulence', which was quite apart from other irrotational motions estimated from surface displacements. From the present results (e.g. Figs. 5 and 6) it is clear that these residual flows result from the difference between the flow of wind waves with a high vorticity region and the flow of simple water waves.

References

BANNER, M.L. and W.K. MELVILLE (1976): On the separation of air flow over water waves. J. Fluid Mech., **77**, 825-842.

GENT, P.E. and P.A. TAYLOR (1977): A note on 'separation' over short wind waves. Boundary-Layer Meteorology, **11**, 65-87.

HATORI, M. (1981): An experimental study of nonlinear processes in the growth of wind waves. Doctoral thesis, Tohoku Univ., 143 pp.

IMASATO, N. and H. ICHIKAWA (1977): Nonlinearity of the horizontal velocity field under wind waves. J. Oceanogr. Soc. Japan, **33**, 61-66.

OKUDA, K. (1982): Internal flow structure of short wind waves. Part I. On the internal vorticity structure. J. Oceanogr. Soc. Japan, **38**, 28-42.

OKUDA, K. (MS): Internal flow structure of short wind waves. Part III. Pressure distributions. J. Oceanogr. Soc. Japan, (in press).

OKUDA, K., S. KAWAI, M. TOKUDA and Y. TOBA (1976): Detailed observation of the wind-exerted surface flow by use of flow visualization methods. J. Oceanogr. Soc. Japan, **32**, 53-64.

PHILLIPS, O.M. (1977): The Dynamics of the Upper Ocean. Cambridge Univ. Press, Cambridge, 336 pp.

TOBA, Y., M. TOKUDA, K. OKUDA and S. KAWAI (1975): Forced convection accompanying wind waves. J. Oceanogr. Soc. Japan, **31**, 192-198.

発達初期の風波の内部構造

第2報 流線パターンについて

奥田邦明*

要旨: 発達初期の風波内部の流れの場の特徴を，特に4つの個々の波について測定した流線に基づいて述べる．第1報ですでに述べたように，いくつかの波においては，峯付近に，その表層に位相速度を越える流れを持つ高渦度領域が形成されている．しかしながら，測定された流線は，水面付近においても，非常に滑らかでかつ規則的なパターンを示した．峯付近の高渦度領域の流れの性質を調べたが，高渦度領域は個々の波において定常的に維持されているのではなく，個々の波の伝播とともに組織的に，顕著な波の崩れを伴うことなく発達，減衰を繰り返していることが明らかとなった．水面付近の渦度層の下では非常に規則的な波動が卓越しているが，この波動は峯付近の高渦度領域の存在により大きな影響を受けている．測定した流線と，個々の波の水面形状から水の波の理論により予想される流線とを比較すると，風波の流れを水位変動から見積ることは，近似的にすら，許されないことが解った．

* 東北大学理学部 〒980 仙台市荒巻字青葉